Inorg. Chem. **2008**, *47*, 11084−11094

Inorganic Chemistry
Article

Synthesis and Characterization of Metallomacrocyclic Palladium(II) Complexes with New Hybrid Pyrazole Ligands. Diffusion NMR Studies and Theoretical Calculations

Miguel Guerrero,[†] Josefina Pons,*[,†] Vicenç Branchadell,[‡] Teodor Parella,[§] Xavier Solans,[||,¶] Mercè Font-Bardia,[||] and Josep Ros*[,†]

Departament de Química, Unitat de Química Inorgànica, Departament de Química, Unitat de Química Física, and Departament de Química i Servei de RMN, Universitat Autònoma de Barcelona, 08193 Bellaterra, Barcelona, Spain, and Cristal·lografia, Mineralogia i Dipòsits Minerals, Universitat de Barcelona, Martí i Franquès s/n, 08028 Barcelona, Spain

Received July 24, 2008

Three new 3,5-dimethylpyrazolic hybrid ligands N1-substituted by polyether chains and phenyl groups have been synthesized: 1,2-bis[4-(3,5-dimethyl-1*H*-pyrazol-1-yl)-2-oxabutyl]benzene (**L1**), 1,3-bis[4-(3,5-dimethyl-1*H*-pyrazol-1-yl)-2-oxabutyl]benzene (**L2**), and 1,4-bis[4-(3,5-dimethyl-1*H*-pyrazol-1-yl)-2-oxabutyl]benzene (**L3**). The reaction of these ligands with $[PdCl_2(CH_3CN)_2]$ gives two kinds of complexes, monomer or dimer, depending on the solvent. Monomeric chelated complexes $[PdCl_2(L)]$ [L = **L1** (**1**), **L2** (**2**), **L3** (**3**)] are obtained when the solvent of the reaction is acetonitrile, whereas when the reaction takes place in tetrahydrofuran binuclear compounds $[PdCl_2(L)]_2$ [L = **L1** (**4**), **L2** (**5**), **L3** (**6**)] are formed. The solid-state structures for **1** and **4** were determined by single-crystal X-ray diffraction methods. All of the palladium(II) complexes **1**−**6** were isolated and fully characterized. Diffusion NMR studies have been performed to characterize monomeric and dimeric species in solution. Dimeric compounds present complex ^{1}H NMR spectra, especially **4**. Theoretical calculations on this molecule suggest that it is due to the coexistence of different conformers that do not interconvert to each other at room temperature. Finally, it has been observed that dimers are converted into the corresponding monomers in an acetonitrile reflux, thus indicating that the latter are thermodynamically more stable than dimers.

Introduction

Supramolecular chemistry has become one of the most interesting fields in modern chemistry. In 1987, Lehn, Pederson, and Cram received the Nobel Prize for their pioneering work.[1] In the last 25 years, supramolecular chemistry has developed at a tremendous rate. This expansion has been driven by the growing knowledge regarding synthetic and characterization methods for complex structures.[2] Furthermore, metallomacrocycles comprise an extremely active area of research that is important for the development of host−guest chemistry, catalysis, receptor site design, and even molecular electronics.[3]

Self-recognition and self-assembly processes represent the basic concept of supramolecular chemistry, and the interactions involved are mainly of a noncovalent nature (e.g., van der Waals, hydrogen-bonding, or ionic interactions). Inter- and intramolecular noncovalent interactions are of major importance for most biological processes.[4]

* To whom correspondence should be addressed. E-mail: Josefina.Pons@uab.es (J.P.), josep.ros@uab.es (J.R.). Fax: 34-93 581 31 01.
[†] Departament de Química, Unitat de Química Inorgànica, Universitat Autònoma de Barcelona.
[‡] Departament de Química, Unitat de Química Física, Universitat Autònoma de Barcelona.
[§] Departament de Química i Servei de RMN, Universitat Autònoma de Barcelona.
[¶] Deceased on September 3, 2007. This paper is dedicated to his memory.
[||] Universitat de Barcelona.

(1) Lehn, J. M. *Supramolecular Chemistry: Concepts and Perspectives*; VCH Publishers: New York, 1995.
(2) (a) Vögtle, F. *Supramolecular Chemistry*; Wiley: Chichester, U.K., 1991. (b) Lehn, J. M. *Comprehensive Supramolecular Chemistry*; Pergamon: New York, 1996. (c) Sun, Q.-F.; Wong, K.; Liu, L.-X.; Huang, H.-P.; Yu, S.-Y.; Yam, V.; Li, Y.-Z.; Pan, Y.-J.; Yu, K.-C. *Inorg. Chem.* **2008**, *47*, 2142–2154.
(3) (a) Lehn, J. M. *Science* **1993**, *260*, 1762–1763. (b) Mirkin, C. A.; Ratner, M. A. *Annu. Rev. Phys. Chem.* **1992**, *43*, 719–754.
(4) (a) Philp, D.; Stoddart, J. F. *Angew. Chem., Int. Ed.* **1996**, *35*, 1155–1196. (b) Darnell, J.; Lodish, H.; Baltimore, B. *Molecular and Cellular Biology*; Scientific American Books: New York, 1990.

10.1021/ic8013915 CCC: $40.75
Published on Web 10/30/2008

Another type of interaction, which is related with our work and has been used extensively in supramolecular chemistry, is metal coordination.[5] Often, this involves the use of metal ions that have defined coordination numbers and stereochemical preferences to encode the rational assembly of specific molecular architectures by recognition of the inherent properties of logically designed ligands.

Through directional coordinative bonding, 2D and 3D self-assemblies are readily available by the spontaneous reaction of metal starting materials with appropriate organic ligands. In 1990, Fujita reported the first example of a metallomacrocycle, a molecular square, synthesized by well-designed metal-directed self-assembly.[6] Recently, this strategy of metal-mediated self-assembly has been successfully applied to construct numerous metallosupramolecular complexes with interesting functions.[7] In this way, many recent reports have described the formation of numerous metallosupramolecular species with novel topological structures, such as squares, cages, ladders, bricks, helicates, and polycatenates.[8] The design of new macrocyclic ligands continues to be an expanding area with the exploration of ring sizes and investigation into various combinations of the donor-atom set (known as "mixed ligands" or "hybrid ligands").[9]

In the last years, our research group has focused its interest on the synthesis and characterization of heterotopic ligands combining a pyrazolyl group with other donor groups with S, N, P, or O and on the study of their reactivity with Zn^{II}, Pd^{II}, Pt^{II}, and Rh^{I}.[10]

In the present work, we describe the synthesis of ligands 1,2-bis[4-(3,5-dimethyl-1*H*-pyrazol-1-yl)-2-oxabutyl]benzene (**L1**), 1,3-bis[4-(3,5-dimethyl-1*H*-pyrazol-1-yl)-2-oxabutyl]benzene (**L2**), and 1,4-bis[4-(3,5-dimethyl-1*H*-pyrazol-1-yl)-2-oxabutyl]benzene (**L3**) and the study of their reactivity toward Pd^{II} in different reaction conditions. Depending on these conditions, two different kinds of complexes have been obtained: monomers and dimers. Both kinds of complexes have been characterized through diffusion NMR studies.

Scheme 1

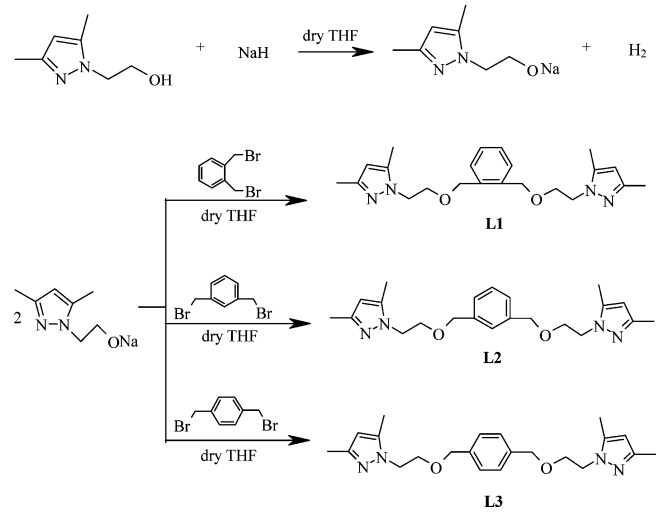

Moreover, for complexes of ligand **L1**, it has been possible to obtain crystals suitable for X-ray diffraction analysis.

Results and Discussion

Synthesis of the Ligands. The synthetic procedure for the preparation of the **L1**−**L3** ligands consists of two steps (Scheme 1). First, 1-(2-hydroxyethyl)-3,5-dimethylpyrazole[11] was reacted with NaH in dry tetrahydrofuran to give the corresponding sodium alkoxide. In the second step, this sodium salt was converted to the corresponding ligand (**L1**, **L2**, or **L3**) by reacting it with the appropriate α,α′-dibromo-***x***-xylene [***x*** = *o* (**L1**), *m* (**L2**), *p* (**L3**)] in dry tetrahydrofuran.

The ligands have been fully characterized by melting point, elemental analysis, mass spectrometry, and IR, ^{1}H and $^{13}C\{^{1}H\}$ NMR spectroscopies. The NMR signals were assigned by reference to the literature[12] and from DEPT, COSY, and HMQC NMR experiments. Elemental analysis,

(5) (a) Constable, E. C. *Chem. Ind.* **1994**, *2*, 56–59. (b) Steel, P. J. *Chem. N. Z.* **2003**, *67*, 57–60. (c) Ward, M. D. *Annu. Rep. Prog. Chem., Sect. A* **2000**, *96*, 345–385. (d) Yu, S.-Y.; Huang, H.-P.; Li, S.-H.; Jiao, Q.; Li, Y.-Z.; Wu, B.; Sei, Y.; Yamaguchi, K.; Pan, Y.-J.; Ma, H.-W. *Inorg. Chem.* **2005**, *44*, 9471–9488.

(6) Fujita, M.; Yakazi, J.; Ogura, K. *J. Am. Chem. Soc.* **1990**, *112*, 5645–5647.

(7) (a) Fujita, M. *Chem. Soc. Rev.* **1998**, *27*, 417–425. (b) Leininger, S.; Olenyuk, B.; Stang, P. J. *Chem. Rev.* **2000**, *100*, 853–907. (c) Swiegers, G. F.; Malefetse, T. J. *Chem. Rev.* **2000**, *100*, 3483–3537. (d) Yoshizawa, M.; Takeyama, Y.; Kusukawa, T.; Fujita, M. *Angew. Chem., Int. Ed.* **2002**, *41*, 1347–1349. (e) Yoshizawa, M.; Takeyama, Y.; Okano, T.; Fujita, M. *J. Am. Chem. Soc.* **2003**, *125*, 3243–3247.

(8) (a) Stang, P. J. *Chem.*—*Eur. J.* **1998**, *4*, 19–27. (b) Lawrence, D. S.; Jiang, T.; Levett, M. *Chem. Rev.* **1995**, *95*, 2229–2260, and references cited therein. (c) Hoskins, B. F.; Robson, R.; Slizys, D. A. *J. Am. Chem. Soc.* **1997**, *119*, 2952–2953. (d) Constable, E. C. *Chem. Commun.* **1997**, *12*, 1073–1080. (e) Baxter, P. N. W.; Lehn, J. M.; Kneisel, B. O.; Fenske, D. *Chem. Commun.* **1997**, *22*, 2231–2232. (f) Fujita, M.; Ogura, K. *Bull. Chem. Soc. Jpn.* **1996**, *69*, 1471–1482. (g) Jones, C. J. *Chem. Soc. Rev.* **1998**, *27*, 289–299. (h) Seel, C.; Vögtle, F. *Angew. Chem., Int. Ed. Engl.* **1992**, *31*, 528–549. (i) Cottam, J. R. A.; Steel, P. J. *Tetrahedron* **2008**, *64*, 2915–2923. (j) Hartshorn, C. M.; Steel, P. J. *Chem. Commun.* **1997**, 541–542.

(9) (a) Würthner, F.; You, C.; Saha-Möller, C. R. *Chem. Soc. Rev.* **2004**, *33*, 133–146. (b) Fallis, I. A. *Annu. Rep. Prog. Chem., Sect. A* **1999**, *95*, 313–351. (c) Steel, P. J. *Molecules* **2004**, *9*, 440–448. (d) Ward, M. D. *Annu. Rep. Prog. Chem., Sect. A* **1999**, *95*, 261–312.

(10) (a) Pañella, A.; Pons, J.; García-Antón, J.; Solans, X.; Font-Bardía, M.; Ros, J. *Eur. J. Inorg. Chem.* **2006**, *8*, 1678–1685. (b) Aullón, G.; Esquius, G.; Lledós, A.; Maseras, F.; Pons, J.; Ros, J. *Organometallics* **2004**, *23*, 5530–5539. (c) Zamora, G.; Pons, J.; Ros, J. *Inorg. Chim. Acta* **2004**, *357*, 2899–2904. (d) Mathieu, R.; Esquius, G.; Lugan, N.; Pons, J.; Ros, J. *Eur. J. Inorg. Chem.* **2001**, *10*, 2683–2688. (e) Esquius, G.; Pons, J.; Yánez, R.; Ros, J.; Mathieu, R.; Donnadieu, B.; Lugan, N. *Eur. J. Inorg. Chem.* **2002**, *11*, 2999–3006. (f) Boixassa, A.; Pons, J.; Solans, X.; Font-Bardía, M.; Ros, J. *Inorg. Chim. Acta* **2004**, *357*, 827–833. (g) Boixassa, A.; Pons, J.; Ros, J.; Mathieu, R.; Lugan, N. *J. Organomet. Chem.* **2003**, *682*, 233–239. (h) Boixassa, A.; Pons, J.; Solans, X.; Font-Bardía, M.; Ros, J. *Inorg. Chim. Acta* **2003**, *355*, 254–263. (i) Rimola, A.; Sodupe, M.; Ros, J.; Pons, J. *Eur. J. Inorg. Chem.* **2006**, *2*, 447–454. (j) García-Antón, J.; Mathieu, R.; Lugan, N.; Pons, J.; Ros, J. *J. Organomet. Chem.* **2004**, *689*, 1599–1608. (k) García-Antón, J.; Pons, J.; Solans, X.; Font-Bardía, M.; Ros, J. *Eur. J. Inorg. Chem.* **2003**, *21*, 3952–3957. (l) Esquius, G.; Pons, J.; Yáñez, R.; Ros, J.; Mathieu, R.; Lugan, N.; Donnadieu, B. *J. Organomet. Chem.* **2003**, *667*, 126–134. (m) Tribó, R.; Muñoz, S.; Pons, J.; Yáñez, R.; Larena, A. A.; Piniella, J. F.; Ros, J. *J. Organomet. Chem.* **2005**, *690*, 4072–4079. (n) Castellano, M. C.; Pons, J.; García-Antón, J.; Solans, X.; Font-Bardía, M.; Ros, J. *Inorg. Chim. Acta* **2008**, *361*, 2923–2928.

(11) Haanstra, W. G.; Driessen, W. L.; Reedijk, J.; Turpeinen, U.; Hämäläinen, R. *J. Chem. Soc., Dalton Trans.* **1989**, *11*, 2309–2314.

(12) (a) Pretsh, E.; Clerc, T.; Seibl, J.; Simon W. Tables of Determination of Organic Compounds. ^{13}C NMR, ^{1}H NMR, IR, MS, UV/Vis, Chemical Laboratory Practice; Springer-Verlag: Berlin, 1989. (b) Williams, D. H.; Fleming, I. *Spectroscopic Methods in Organic Chemistry*; McGraw-Hill: London, 1995.

Scheme 2

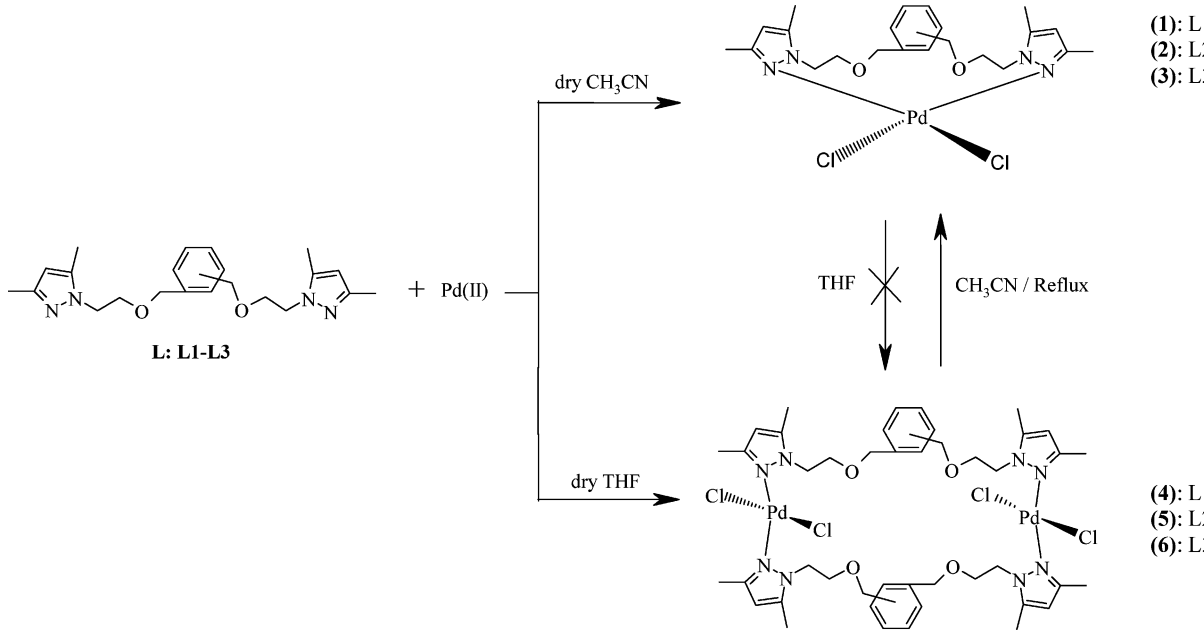

mass spectrometry, and all spectroscopic data for **L1**, **L2**, and **L3** are consistent with the proposed structures.

Synthesis and Characterization of the Complexes. The reaction of ligands **L1**−**L3** with Pd^{II} in dichloromethane in a 1:1 M/L ratio yields a mixture of two compounds. This mixture has been characterized essentially by 1D and 2D NMR techniques. ^{1}H NMR spectra indicate the presence of two types of compounds: one species with a well-defined signal multiplicity and another one with a higher and more complex multiplet pattern. Furthermore, the corresponding DOSY spectra clearly indicate the existence of two different-sized species that strongly agree with the presence of the monomeric and dimeric complexes.

Several procedures have been tried to obtain pure monomeric and dimeric complexes. First, we have tried to separate them by recrystallization, chromatography, and extraction. We have also modified the synthetic procedure, changing the temperature and/or time of the reaction and the M/L molar ratio. Finally, the best results were obtained by changing the solvent. In this way, the reaction between ligands **L1**−**L3** and Pd^{II} gives two types of compounds, monomers and dimers, depending upon the solvent (Scheme 2). Monomeric complexes $[PdCl_2(L)]$ [L = **L1** (**1**), **L2** (**2**), **L3** (**3**)] were obtained by treatment of the corresponding ligand with $[PdCl_2(CH_3CN)_2]$[13] in a 1:1 M/L ratio in CH_3CN for 12 h at room temperature (**1**), 24 h at 60 °C (**2**), or 168 h at 70 °C (**3**). On the other hand, dimeric complexes $[PdCl_2(L)]_2$ [L = **L1** (**4**), **L2** (**5**), **L3** (**6**)] were obtained by treatment of the corresponding ligand with $[PdCl_2(CH_3CN)_2]$ in a 1:1 M/L ratio in tetrahydrofuran for 12 h at room temperature.

The elemental analyses for complexes **1**−**6** are consistent with the formula $[PdCl_2(L)]$ [L = **L1** (**1** and **4**), **L2** (**2** and **5**), or **L3** (**3** and **6**)]. The positive ionization spectra (ESI^+-MS) of compounds **1**−**3** give a peak with a value of *m*/*z* 525.3 (100%) attributable to $[PdCl(L)]^+$, and for compounds **4**−**6**, a peak with a value of *m*/*z* 1083.2 (100%) attributable to $[Pd_2Cl_3(L)]^+$ is observed. Molecular peaks of the cations are observed with the same isotope distribution as the theoretical one, as shown for complex **4** (Figure 1). Conductivity values in acetonitrile for all complexes are in agreement with the presence of nonelectrolyte compounds (8.5−13.2 S cm^2 mol^{-1}). The reported values for 10^{-3} M solutions in acetonitrile of nonelectrolyte complexes are lower than 120 S cm^2 mol^{-1}.[14]

The IR spectra of complexes **1**−**6** in the range 4000−400 cm^{-1} show that the ligands are coordinated to Pd^{II}. The ν(C═C), ν(C═N), and $\delta(C-H)_{oop}$ bands of the pyrazolic ligands increase their frequencies when they are part of the complexes. The most characteristic bands in the IR spectra between 4000 and 400 cm^{-1} are those attributable to the pyrazolyl, phenyl, and ether groups.[12] The IR spectra of complexes **1**−**6** in the 600−100 cm^{-1} region were also studied. The presence of bands between 494 and 471 cm^{-1} assigned to ν(Pd−N) confirms the coordination of the N_{pz} of the ligand to the metallic atom. All of the complexes display a ν(Pd−Cl) band between 355 and 335 cm^{-1}. This band indicates that the chlorine atoms are coordinated to Pd^{II} in a trans disposition.[15]

Moreover, for complexes **1** and **4**, which incorporate the ligand **L1**, it has been possible to obtain crystals suitable for X-ray analyses. The molecular structure of monomeric complex **1** (Figure 2) consists of Pd^{II} discrete molecules with a slightly distorted square-planar geometry around the metal atom. The environment consists of two chlorine atoms in a trans disposition to the Pd^{II} and two nitrogen atoms of the pyrazolic rings of **L1**. The N1−Pd−N4 and Cl2−Pd−Cl1

(13) Komiya, S. *Synthesis of Organometallic Compounds: A Practice Guide*; Board: New York, 1997.

(14) (a) Geary, W. J. *Coord. Chem. Rev.* **1971**, *7*, 81–122. (b) Thompson, L. K.; Lee, F. L.; Gabe, E. J. *Inorg. Chem.* **1988**, *27*, 39–46.

(15) Nakamoto, K. *Infrared and Raman Spectra of Inorganic and Coordination Compounds*; John Wiley and Sons: New York, 1986.

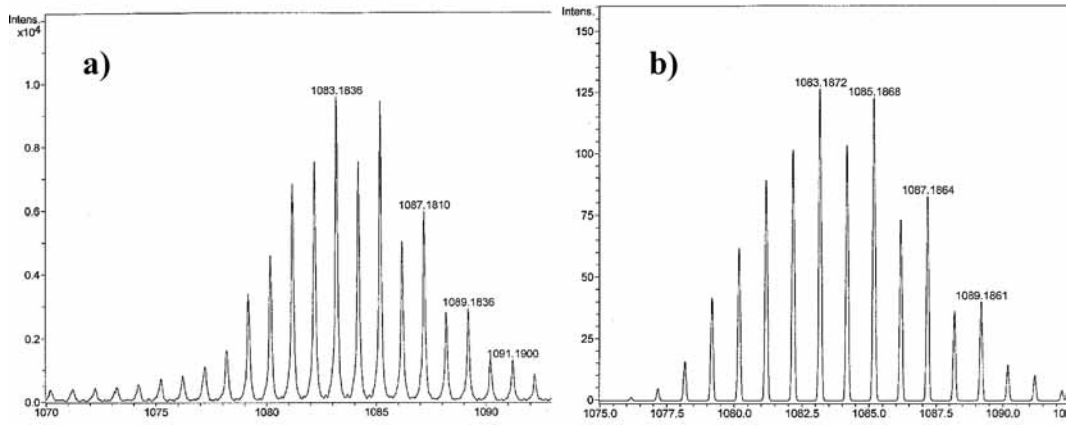

Figure 1. (a) ESI^+-MS spectra in methanol of fragments $[Pd_2Cl_3(\mathbf{L1})]^+$ for complex **4** and (b) theoretical isotopic distribution of **4**.

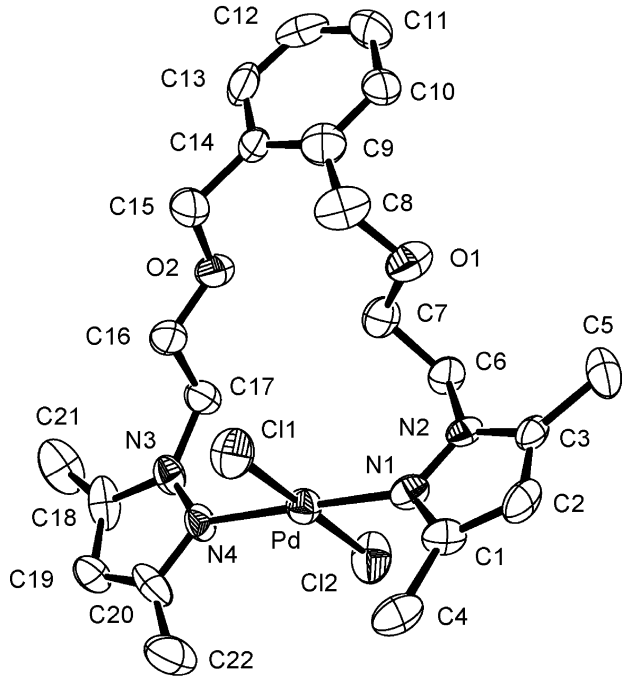

Figure 2. ORTEP diagram of complex **1** showing an atom labeling scheme. 50% probability amplitude displacement ellipsoids are shown. Hydrogen atoms are omitted for clarity. See Table 1 for selected values of the bond lengths and bond angles.

angles are 178.4(3)° and 178.62(9)°, respectively, showing a slight tetrahedral distortion. This distortion can also be observed from the deviation [0.024(2) Å] of Pd^{II} from the mean plane (N1, N4, Cl1, and Cl2). **L1**, which acts as a bidentate chelate ligand, forms a metallocycle ring of 15 members. The $[PdCl_2(N_{pz})_2]$ *core*, with a bidentate chelate ligand, is present in 12 complexes in the literature.[16] Only one of these structures presents the chlorine atoms in a trans disposition.[17] Selected values of the bond lengths and bond angles for complex **1** are shown in Table 1. The Pd−Cl and $Pd-N_{pz}$ bond distances are in agreement with the values reported in the literature (2.220−2.361 and 1.979−2.141 Å,

Table 1. Selected Bond Lengths (Å) and Bond Angles (deg) for **1** and **4**

	1	**4**
Pd−N1	1.993(6)	1.985(5)
Pd−N4	2.014(6)	1.988(5)
Pd−Cl2	2.303(2)	2.225(11)
Pd−Cl1	2.306(2)	2.286(3)
N1−Pd−N4	178.4(3)	173.9(2)
N1−Pd−Cl2	89.79(17)	90.2(3)
N4−Pd−Cl2	90.91(19)	87.0(3)
N1−Pd−Cl1	89.34(17)	91.65(17)
N4−Pd−Cl1	89.94(19)	91.75(17)
Cl2−Pd−Cl1	178.62(9)	172.79(16)

respectively),[17,18] and the N−Pd−N and Cl−Pd−Cl angles are within the expected range for monomeric palladium(II) compounds with a square-planar geometry.

The crystal structure of complex **4** (Figure 3) consists of Pd^{II} discrete dimeric molecules and two molecules of water, one of them with severe disorder. Complex **4** lies on a crystallographic inversion center. Moreover, the structure has a distorted square-planar geometry around the metal atom. The environment consists of two chlorine atoms coordinated in a trans disposition (one of them with severe disorder) to the Pd^{II} and two nitrogen atoms of the pyrazolic rings of **L1**. The N1−Pd−N4 and Cl2−Pd−Cl1 angles are 173.9(2)° and 172.79(16)°, respectively, showing a higher tetrahedral distortion than complex **1**. It can also be observed from the larger deviation [0.085(2) Å] of the Pd^{II} from the mean plane (N1, N4, Cl1, and Cl2). Contrary to what we have found for complex **1**, **L1** acts in complex **4** as a bidentate bridge ligand and forms a homobimetallic macrocycle of 30 members. The $[Pd_2Cl_4(N_{pz})_4]$ *core* (where the ligand acts as a bidentate and a bridge) is present in two complexes in the literature.[19] The most similar crystal structure corresponds

(16) Allen, F. A. *Acta Crystallogr.* **2002**, *B58*, 380–388.
(17) García-Antón, J.; Pons, J.; Solans, X.; Font-Bardía, M.; Ros, J. *Eur. J. Inorg. Chem.* **2002**, *12*, 3319–3327.
(18) (a) García-Antón, J.; Pons, J.; Solans, X.; Font-Bardía, M.; Ros, J. *Inorg. Chim. Acta* **2003**, *355*, 87–94. (b) Boixassa, A.; Pons, J.; Solans, X.; Font-Bardía, M.; Ros, J. *Inorg. Chim. Acta* **2003**, *346*, 151–157. (c) Boixassa, A.; Pons, J.; Solans, X.; Font-Bardía, M.; Ros, J. *Inorg. Chim. Acta* **2004**, *357*, 733–738. (d) Torralba, M. C.; Cano, M.; Campo, J. A.; Heras, J. V.; Pinilla, E. *Z. Kristallogr.: New Cryst. Struct.* **2005**, *220*, 617–619. (e) Montoya, V.; Pons, J.; Solans, X.; Font-Bardía, M.; Ros, J. *Inorg. Chim. Acta* **2006**, *359*, 25–34. (f) Spencer, L. C.; Guzei, I. A.; Ojwach, S. O.; Darkwa, J. *Acta Crystallogr., Sect. C: Cryst. Struct. Commun.* **2006**, *62*, m421−m423.
(19) (a) Jouaiti, A.; Hosseini, M. W.; Kyritsakas, N. *Eur. J. Inorg. Chem.* **2003**, *1*, 57–61. (b) Motsoane, N. M.; Guzei, I. A.; Darkwa, J. *Z. Naturforsch., B: Chem. Sci.* **2007**, *62*, 323–330.

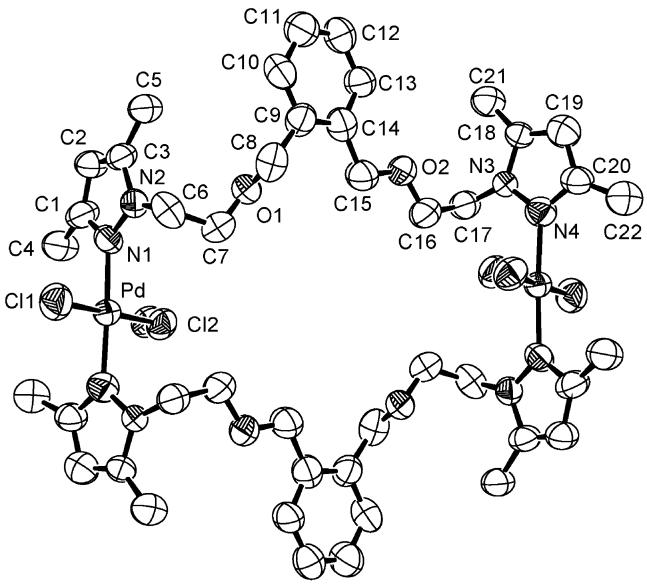

Figure 3. ORTEP diagram of complex **4** showing an atom labeling scheme. 50% probability amplitude displacement ellipsoids are shown. Solvents molecules and hydrogen atoms are omitted for clarity. The chlorine atoms (Cl2) are disordered. See Table 1 for selected values of the bond lengths and bond angles.

to the complex $[Pd_2Cl_4(L)_2]$ [L = 1,2-bis(3,5-dimethylpyrazol-1-ylmethyl)benzene], a macrocycle of 18 members.[19b] Selected bond lengths and bond angles for complex **4** are shown in Table 1. As in complex **1**, the Pd−Cl and Pd−N_{pz} bond distances and the N−Pd−N and Cl−Pd−Cl angles in complex **4** are typical of palladium(II) square-planar complexes and are in agreement with the values reported in the literature.[17−19] Both the average Pd−Cl and Pd−N_{pz} distances are longer for complex **1** than those in **4**. The intramolecular Pd···Pd separation in the macrocycle is 11.499-(2) Å. This value is significantly larger than the values found in the literature for $[Pd_2Cl_4(N_{pz})_4]$ [7.691(3) Å].[19b] The two benzene rings are parallel planar but do not overlap (their centroids are displaced by over 11 Å) and therefore do not exhibit evidence of intramolecular $\pi-\pi$ interaction in the solid state. This also indicates that the dimension of the macrocycle is enlarged from the earlier structure.[19b]

In this complex, the ether moieties do not coordinate to Pd^{II}, so these can be envisaged to be applied in host−guest chemistry because of the similarity with the heterocrown ether.[20]

The presence of monomeric and dimeric complexes in solution has also been evidenced through diffusion NMR experiments in CD_3CN for all of the complexes. These experiments are a powerful method to provide information about the relative size of the molecules in solution.[21] The Stokes−Einstein equation (eq 1) shows that a sphere's diffusion coefficient (D) is inversely related to its hydrodynamic radius (R_H) and solvent viscosity (η).

$$D = \frac{k_B T}{6\pi\eta R_H} \quad (1)$$

Thus, the ratio of diffusion rates for two different spherical molecules in the same environment is inversely proportional to the ratio of their radii and, therefore, their relative molecular sizes in solution may be estimated from measurement of the diffusion rates (eq 2).

$$\frac{D_{monomer}}{D_{dimer}} = \frac{R_{dimer}}{R_{monomer}} \quad (2)$$

Measurement of the diffusion coefficients was made from DOSY spectra of a mixture of compounds **1** and **4** at 298 K in a CD_3CN solution, and the obtained results are shown in Figure 4. The monomer **1** (MW = 559.8 g mol^{-1}) presents a D value of $(11.2 \pm 0.09) \times 10^{-10}$ m^2 s^{-1} that is equivalent to a hydrodynamic radius of 6.43 ± 0.60 Å. In contrast, the dimer **4** (MW = 1119.6 g mol^{-1}) has a D value of (8.70 ± 0.09) × 10^{-10} m^2 s^{-1}, with R_H of 8.28 ± 0.60 Å. These hydrodynamic radii are in qualitative agreement with the crystal structural radii (R_E; 6.25 and 8.88 Å for **1** and **4**, respectively). Similar D values were obtained for **2/5** and **3/6** mixtures (see the Supporting Information). Assuming that both dimer and monomer derivatives present similar shapes, the predicted ratio between their radii should be about 1.26. This value is in close analogy to the ratios obtained experimentally: 1.29 for **1/4**, 1.32 for **2/5**, and 1.28 for **3/6**.

As we have shown, for **L1**−**L3** ligands, monomeric and dimeric palladium(II) complexes coexist in a CD_3CN solution, and they have been fully characterized by 1D and 2D NMR spectroscopy. However, no interconversion between them could be observed on the NMR time scale from resonance line-shape changes in variable-temperature ^1H spectra or by the presence of exchange cross-peaks in NOESY spectra (253−323K). In general, the signals in the ^1H NMR spectra for all complexes appear at lower fields than free ligands, especially for the $N_{pz}CH_2CH_2O$ fragment because of their proximity to the nitrogen-coordinated atom in the chain. The ^1H NMR spectra of dimeric complexes **4**−**6** are much more complicated than those of monomers **1**−**3**. This is especially evident if we compare the spectra of **1** and **4** (see Figure 5). As we can observe, for complex **4**, all of the ^1H NMR resonances show complicated multiplet patterns, probably because of the presence of different stable conformers with significant population in the 253−323 K temperature range. These conformers would only be interchangeable through high-energy barriers.[22] For this reason, theoretical calculations have been carried out.

Theoretical Calculations. We have studied the monomeric and dimeric complexes of ligand **L1** (**1** and **4**, respectively) because **4** is the complex with the most complex ^1H NMR spectrum. For the monomer **1**, we have obtained three different conformers, which differ from each other in

(20) (a) Tsukube, H. *Coord. Chem. Rev.* **1996**, *148*, 1–17. (b) Schäfer, M. *Angew. Chem., Int. Ed.* **2003**, *42*, 1896–1899.

(21) Valentini, M.; Rüegger, H.; Pregosin, P. S. *Organometallics* **2000**, *19*, 2551–2555.

(22) (a) Bain, A. D.; Bell, R. A.; Fletcher, D. A.; Hazendonk, P.; Maharajh, R. A.; Rigby, S.; Valliant, J. F. *J. Chem. Soc., Perkin Trans. 2* **1999**, *7*, 1447–1453. (b) Jackman, L. M.; Cotton, F. A. *Dynamic Nuclear Magnetic Resonance Spectroscopy*; Academic Press: New York, 1975. (c) Buevich, A. V.; Chan, T.-M.; Wang, C. H.; McPhail, A. T.; Ganguly, A. K. *Magn. Reson. Chem.* **2005**, *43*, 187–199.

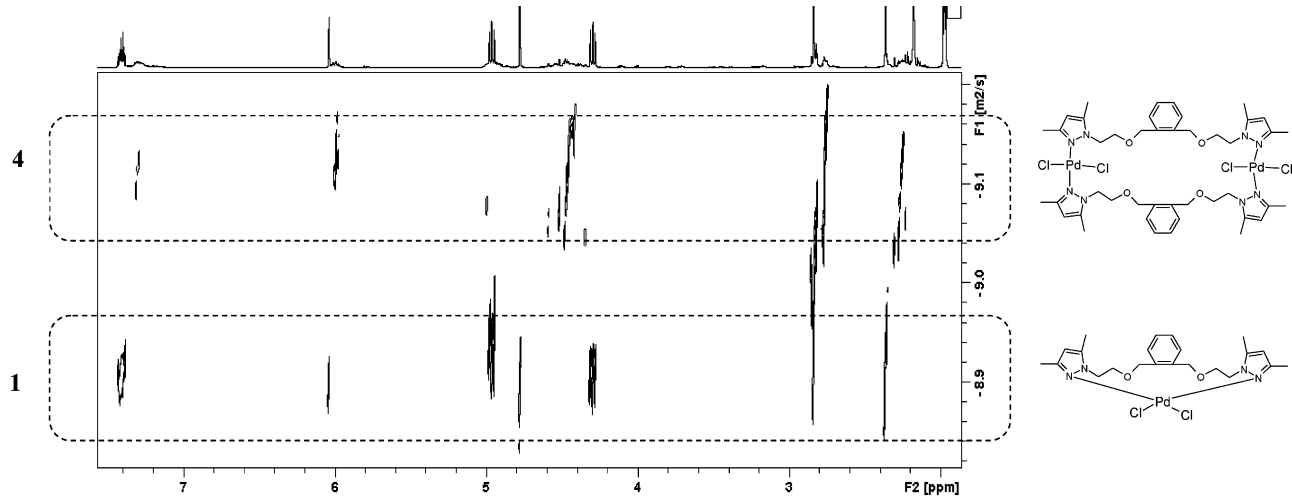

Figure 4. Expanded area of the DOSY spectrum (500 MHz, 298 K, tetramethylsilane) of a mixture of monomer (**1**) and dimer (**4**) in CD_3CN.

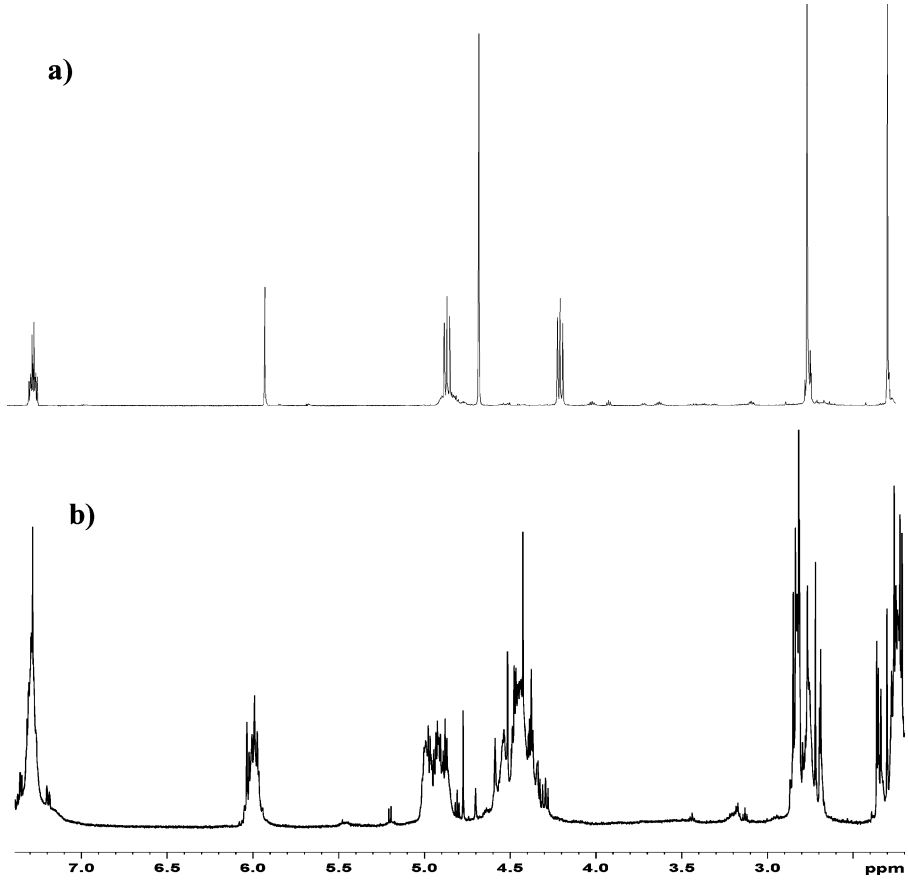

Figure 5. ^1H NMR spectrum (250 MHz, 298 K, tetramethylsilane) in CD_3CN of (a) complex **1** and (b) complex **4**.

the dihedral angles around C8−O1, C7−C6, C15−O2, and C16−C17. The structures of the two most stable conformers are shown in Figure 6. The most stable conformer **1-I** is the one corresponding to the X-ray structure. The second most stable conformer **1-II** is 1.2 kcal mol^{-1} above **1-I** and differs from it in the torsion angles around C8−O1 and C7−C6, which present a gauche disposition (dihedral angles −73.9° and 65.8°, respectively) in **1-I**, whereas in **1-II**, they are trans (dihedral angles −167.8° and −177.4°, respectively). The estimated population ratio between conformers **1-I** and **1-II** at 298 K is 89:11. The third conformer **1-III**, which is 4.5 kcal mol^{-1} above **1-I**, is not expected to be populated at room temperature, and its structure can be found in the Supporting Information.

For the dimeric complex **4**, we have obtained eight different conformers in a range of 5.8 kcal mol^{-1}. Figure 7 shows the structures of the five most stable conformers. The structures of the other three conformers can be found as Supporting Information. Table 3 presents the relative energies of all conformers as well as the values of the most significant dihedral angles for each conformer. The structure of the most stable conformer is also presented in Figure 8 along with atom numbering. It is to be noted that the most stable conformer does not correspond to the X-ray structure. The

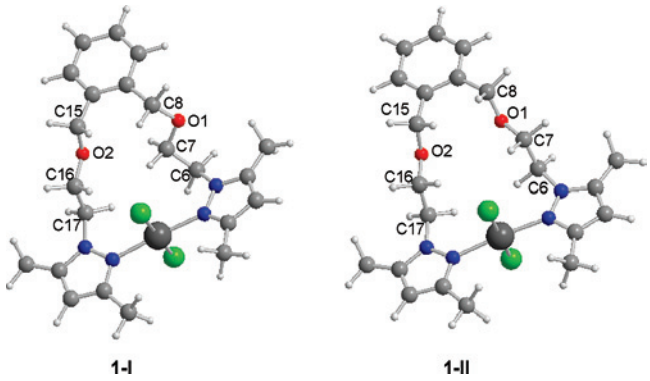

Figure 6. Structure of the two most stable conformers of **1** obtained at the BPW91/LANL2DZ(d) level of calculation.

conformer similar to the X-ray structure is **4-V** and lies 3.4 kcal mol^{-1} above the most stable one. Conformers **4-I** and **4-II** differ from each other in the dihedral angles around C16−C17, C17−N3, C16′−C17′, and C17′−N3′. In both conformers, these dihedral angles correspond to gauche arrangements. The interconversion between **4-I** and **4-II** would involve eclipsed conformations (dihedral angles around 0°). Such rearrangements are expected to be very unfavorable because of the macrocyclic nature of **4**. For this reason, both conformers would not interconvert to each other in solution. The third conformer, **4-III**, differs from **4-II** in the torsion angles around C14−15 and C14′−C15′', which change from an anti to a gauche disposition. Such a rearrangement would also involve eclipsed conformations. In conformer **4-IV**, dihedral angles around O2−C16 and O2′−C16′ adopt values of around +110° and −120°, respectively, in contrast to values around 180° for the first three conformers. The values of these two dihedral angles are the only significant variation between conformers **4-III** and **4-IV**, so that their interconversion should not involve a very high energy barrier. For the first four conformers, both ligands adopt nearly the same conformation, whereas for **4-V**, this is not the case. This conformer differs from the most stable one in the dihedral angles around C14−C15, O2−C16, C7′−O1, and C8′−C9′, which change from anti in **4-I** to gauche in **4-V**. Such rearrangements are also expected to involve high-energy barriers.

According to these results, in addition to the conformer corresponding to the X-ray structure (**4-V**), there are four other conformers with lower energies. At least these five conformers could coexist in solution at room temperature. With the exception of conformers **4-III** and **4-IV**, conformational rearrangements are expected to involve high-energy barriers because of the restrictions imposed by the macrocyclic nature of complex **4**, and the possible interconversion between conformers probably would take place through metal−ligand bond cleavage. Starting from conformer **4-I**, we have optimized a structure in which one of the Pd−N bonds has been broken and its energy is 33.4 kcal mol^{-1} above **4-I**. This value may provide an approximation to the energy barrier associated with interconversion between conformers. As a consequence, these conformers would not be in equilibrium in solution at room temperature. These results are compatible with a complex ^{1}H NMR spectrum, such as the one shown in Figure 5.

Conversion of Binuclear Complexes to Mononuclear Complexes. The conversion of the dimeric complexes **4**−**6** into the analogous mononuclear complexes **1**−**3** has been studied (Scheme 2). Similar conversions have been observed for other systems.[23] The conversion was monitored by ^{1}H NMR spectroscopy with no sign of decomposition or side reactions except in complex **6**, because of its difficulty to form the respective monomer complex **3** (strain of the cycle). The conversion was studied in a CH_3CN reflux to obtain the thermodynamically favored product in these conditions, complexes **1** (24 h), **2** (40 h), and **3** (120 h). On the other hand, dimerization of the monomeric complexes in tetrahydrofuran has not been observed.

Theoretical calculations show that the dimerization of **1** to form **4** is energetically favorable ($\Delta E = -4.9$ kcal mol^{-1}), but entropy makes the process thermodynamically unfavorable at 25 °C ($\Delta G° = 7.2$ kcal mol^{-1}). This result is consistent with the dimer decomposition observed in an acetonitrile reflux.

Conclusion

In the present work, we have synthesized three pyrazole ether ligands and studied the reactivity toward Pd^{II} in different solvents. Two kinds of complexes have been obtained: monomeric $[PdCl_2(L)]$ and dimeric macrocyclic $[PdCl_2(L)]_2$ complexes depending on the solvent. The solid-state structures for **1** and **4** were determined by single-crystal X-ray diffraction methods. Monomeric and dimeric complexes in solution have been characterized through diffusion NMR studies. Dimeric compounds present complex ^{1}H NMR spectra, especially **4**, and theoretical calculations suggest the coexistence of different conformers that do not interconvert into each other at room temperature. Finally, it has been observed that dimers are converted into the corresponding monomers in an acetonitrile reflux, thus indicating that the latter are thermodynamically more stable than dimers.

Experimental Section

General Procedures. Unless otherwise noted, all reactions and manipulations were carried out under an atmosphere of dry nitrogen using vacuum-line and standard Schlenk techniques. All solvents were dried and distilled according to standard procedures and stored under nitrogen.[24] Samples of $[PdCl_2(CH_3CN)_2]$ were prepared as described in the literature.[13]

Instrumentation. Melting points were measured on a Electrothermal 1A8104 melting point apparatus. Elemental analyses (C, H, and N) were carried out by the staff of Chemical Analyses Service of the Universitat Autònoma de Barcelona on a Eurovector 3011 instrument. Conductivity measurements were performed at room temperature in 10^{-3} M CH_3CN solutions, employing a

(23) (a) Hollyday, B. J.; Mirkin, C. A. *Angew. Chem., Int Ed.* **2001**, *40*, 2022–2043. (b) Farrell, J. R.; Eisenberg, A. H.; Mirkin, C. A.; Guzei, I. A.; Liable-Sands, L. M.; Incarvito, C. D.; Rheingold, A. L.; Stern, C. L. *Organometallics* **1999**, *18*, 4856–4868.

(24) Armarego, W. L. F.; Perrin, D. *Purification of Laboratory Chemicals*; Butterworth-Heinemann: Oxford, U.K., 1996.

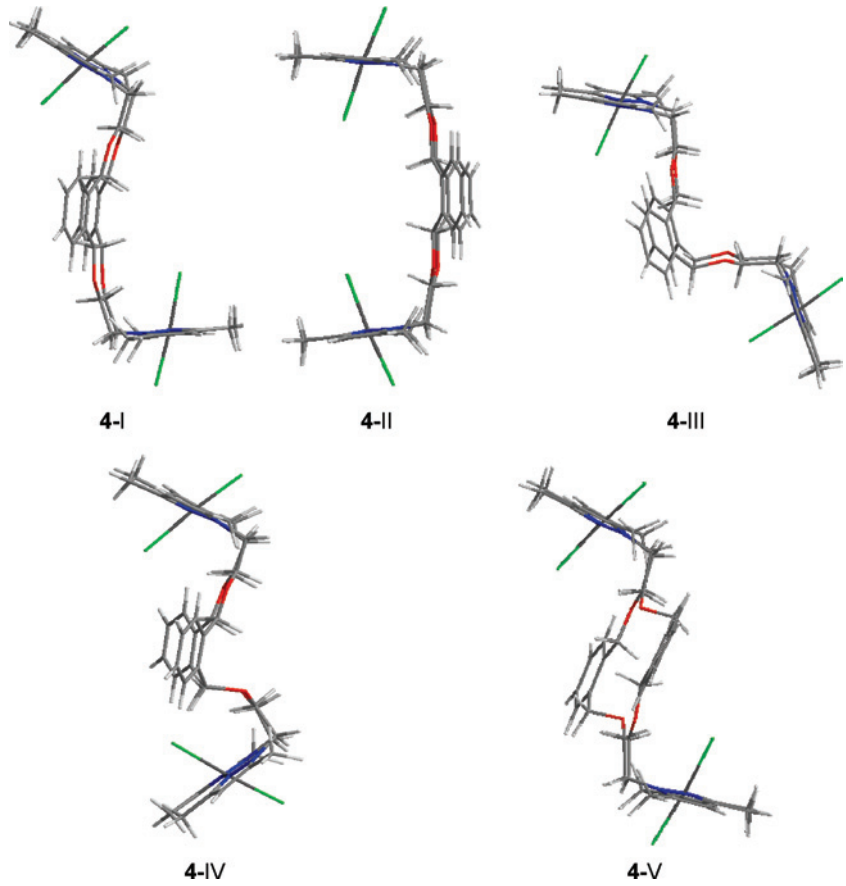

Figure 7. Structure of the five most stable conformers of **4** obtained at the BPW91/LANL2DZ(d) level of calculation.

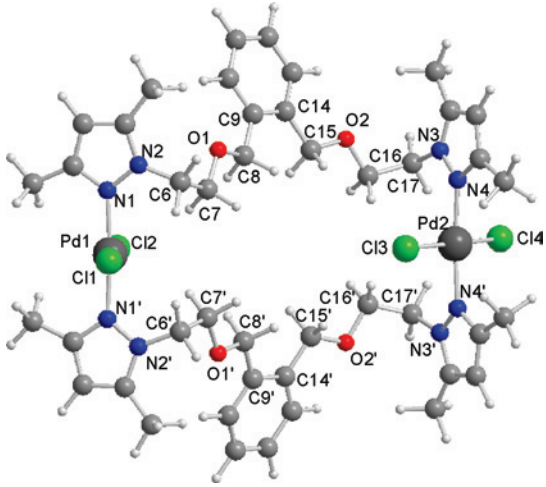

Figure 8. Structure and atom numbering for the most stable conformer of **4** (**4-I**) obtained at the BPW91/LANL2DZ(d) level of calculation.

CyberScan CON 500 (Eutech instrument) conductimeter. IR spectra were run on a Perkin-Elmer FT spectrophotometer series 2000 cm^{-1} as KBr pellets or polyethylene films in the range 600−100 cm^{-1}. ^1H, $^{13}C\{^1H\}$, 2D HMQC, 2D COSY, and 2D NOESY NMR spectra were recorded on a Bruker 250 MHz AVANCE spectrometer in $CDCl_3$ or CD_3CN solutions at room temperature. NMR diffusion experiments were carried out at 298 K on a 500 MHz AVANCE spectrometer equipped with a 5 mm TCI cryoprobe. Self-diffusion experiments were performed using the compensated BPLED pulse sequence[25] in order to avoid unwanted convection effects, using a diffusion time of 150 ms and a LED delay of 5 ms. For each experiment, sine-shaped pulsed-field gradients with a duration of 1.5 ms followed by a recovery delay of 100 μs were incremented from 2% to 95% of the maximum strength in 16 equally spaced steps. Diffusion coefficients were obtained by measurement of the slope in the following linear relationship: $\ln(A_g/A_0) = -\gamma^2 g^2 \delta^2 (4\Delta - \delta)D$, where A_g and A_0 are the signal intensities in the presence and absence of a pulsed-field gradient, respectively, γ is the gyromagnetic ratio (rad s g^{-1}), g is the strength of the diffusion gradients (G cm^{-1}), D is the diffusion coefficient of the observed spins (m^2 s^{-1}), δ is the length of the diffusion gradient (s), and Δ is the time separation between the leading edges of the two diffusion pulsed gradients (s). All chemical shift values (δ) are given in ppm. Electrospray mass spectra were obtained with an Esquire 3000 ion-trap mass spectrometer from Bruker Daltonics.

Computational Details. All calculations have been done using the *Gaussian-03* program.[26] The geometries have been fully optimized using the BPW91[27,28] density functional with the LANL2DZ basis set supplemented with d polarization functions for C, N, and O [LANL2DZ(d)]. This basis set uses effective core potentials for Pd[29] and the D95 basis set for the remaining atoms.[30] For the most stable conformer of each complex, harmonic vibrational frequencies have been computed.

(25) Jerschow, A.; Muller, N. *J. Magn. Reson.* **1997**, *125*, 372–375.

(26) Frisch, M. J.; et al. *Gaussian 03*, revision C.02; Gaussian, Inc.: Wallingford CT, 2004; http://www.gaussian.com.

(27) Becke, A. D. *Phys. Rev. A* **1988**, *38*, 3098–3100.

(28) (a) Wang, Y.; Perdew, J. P. *Phys. Rev. B* **1991**, *44*, 13298–13301. (b) Perdew, J. P.; Chevary, J. A.; Vosko, S. H.; Jackson, K. A.; Pederson, M. R.; Singh, D. J.; Fiolhais, C. *Phys. Rev. B* **1992**, *46*, 6671–6687.

(29) (a) Hay, P. J.; Wadt, W. R. *J. Chem. Phys.* **1985**, *82*, 270–283. (b) Wadt, W. R.; Hay, P. J. *J. Chem. Phys.* **1985**, *82*, 284–298.

(30) Dunning, T. H.; Hay, P. J. In *Modern Theoretical Chemistry*; Schaeffer, H. F., III, Ed.; Springer: New York, 1976; Vol. *3*.

Synthesis of the Ligands L1, L2, and L3. A solution of 2.80 g (0.020 mol) of 1-(2-hydroxyethyl)-3,5-dimethylpyrazole in 50 mL of tetrahydrofuran was slowly added to a suspension of 0.53 g (0.022 mol) of NaH in 10 mL of tetrahydrofuran. The solution was stirred at 60 °C for 2 h. A total of 2.75 g (0.010 mol) of α,α′-dibromo-***x***-xylene [***x*** = *o* (**L1**), *m* (**L2**), *p* (**L3**)] in 10 mL of tetrahydrofuran was added dropwise and under vigorous stirring. The resulting mixture was allowed to stir for 12 h at 60 °C. After cooling to room temperature, 10 mL of water was added dropwise to destroy excess NaH. The solvents were then evaporated under reduced pressure. The residue was taken up in water (40 mL) and extracted with chloroform (3−50 mL). The chloroform layers were dried with anhydrous $MgSO_4$ and evaporated.

L1. Yield: 62% (2.37 g). Mp: 64.8−65.3 °C. Anal. Calcd for $C_{22}H_{30}N_4O_2$: C, 69.08; H, 7.91; N, 14.65. Found: C, 69.29; H, 8.02; N, 14.67. MS: *m*/*z* 383.2 (100%) $[M + H]^+$. IR (KBr, cm^{-1}): 3052 [ν(C−H)$_{ar}$], 2929, 2869 [ν(C−H)$_{al}$], 1553 [ν(C═C), ν(C═N)$_{ar}$], 1423 [δ(C═C), δ(C═N)$_{ar}$], 1104 [ν(C−O−C)$_{as}$], 736, 703 [δ(C−H)$_{oop}$]. ^{1}H NMR ($CDCl_3$ solution, 250 MHz): δ 7.19 (s, 4H, Ph), 5.80 (s, 2H, C*H*(pz)), 4.44 (s, 4H, OCH_2Ph), 4.12 (t, 4H, ^3J = 5.6 Hz, $N_{pz}CH_2CH_2O$), 3.71 (t, 4H, ^3J = 5.6 Hz, $N_{pz}CH_2CH_2O$), 2.22 (s, 12H, CH_3(pz)). ^{13}C{^{1}H} NMR ($CDCl_3$ solution, 63 MHz): δ 147.9 (pz-*C*), 140.2 (pz-*C*), 137.9−127.7 (Ph), 105.1 (*C*H(pz)), 73.2 (O*C*H$_2$Ph), 69.7 ($N_{pz}CH_2CH_2O$), 48.8 ($N_{pz}CH_2CH_2O$), 13.9 (*C*H$_3$(pz)), 11.4 (*C*H$_3$(pz)).

L2. Yield: 74% (2.83 g). Mp: 68.1−69.3 °C. Anal. Calcd for $C_{22}H_{30}N_4O_2$: C, 69.08; H, 7.91; N, 14.65. Found: C, 68.89; H, 7.64; N, 14.48. MS: *m*/*z* 383.2 (100%) $[M + H]^+$. IR (KBr, cm^{-1}): 3016 [ν(C−H)$_{ar}$], 2920, 2863 [ν(C−H)$_{al}$], 1553 [ν(C═C), ν(C═N)$_{ar}$], 1425 [δ(C═C), δ(C═N)$_{ar}$], 1111 [ν(C−O−C)$_{as}$], 778, 702 [δ(C−H)$_{oop}$]. ^{1}H NMR ($CDCl_3$ solution, 250 MHz): δ 7.31 (m, 1H, Ph), 7.19 (s, 2H, Ph), 7.15 (m, 1H, Ph), 5.81 (s, 2H, C*H*(pz)), 4.47 (s, 4H, OCH_2Ph), 4.16 (t, 4H, ^3J = 5.2 Hz, $N_{pz}CH_2CH_2O$), 3.81 (t, 4H, ^3J = 5.2 Hz, $N_{pz}CH_2CH_2O$), 2.27 (s, 6H, CH_3(pz)), 2.22 (s, 6H, CH_3(pz)). ^{13}C{^{1}H} NMR ($CDCl_3$ solution, 63 MHz): δ 147.1 (pz-*C*), 139.5 (pz-*C*), 138.4−126.6 (Ph), 104.4 (*C*H(pz)), 72.8 (O*C*H$_2$Ph), 69.3 ($N_{pz}CH_2CH_2O$), 48.4 ($N_{pz}CH_2CH_2O$), 13.1 (*C*H$_3$(pz)), 10.7 (*C*H$_3$(pz)).

L3. Yield: 65% (2.48 g). Mp: 69.2−71.1 °C. Anal. Calcd for $C_{22}H_{30}N_4O_2$: C, 69.08; H, 7.91; N, 14.65. Found: C, 69.18; H, 7.99; N, 14.72. MS: *m*/*z* 383.2 (100%) $[M + H]^+$. IR (KBr, cm^{-1}): 3026 [ν(C−H)$_{ar}$], 2981, 2863 [ν(C−H)$_{al}$], 1552 [ν(C═C), ν(C═N)$_{ar}$], 1427 [δ(C═C), δ(C═N)$_{ar}$], 1101 [ν(C−O−C)$_{as}$], 774 [δ(C−H)$_{oop}$]. ^{1}H NMR ($CDCl_3$ solution, 250 MHz): δ 7.16 (s, 4H, Ph), 5.78 (s, 2H, C*H*(pz)), 4.42 (s, 4H, OCH_2Ph), 4.14 (t, 4H, ^3J = 5.2 Hz, $N_{pz}CH_2CH_2O$), 3.78 (t, 4H, ^3J = 5.2 Hz, $N_{pz}CH_2CH_2O$), 2.23 (s, 6H, CH_3(pz)), 2.21 (s, 6H, CH_3(pz)). ^{13}C{^{1}H} NMR ($CDCl_3$ solution, 63 MHz): δ 147.6 (pz-*C*), 139.9 (pz-*C*), 136.1−128.0 (Ph), 104.9 (*C*H(pz)), 70.7 (OCH_2Ph), 69.4 ($N_{pz}CH_2CH_2O$), 48.6 ($N_{pz}CH_2CH_2O$), 13.5 (*C*H$_3$(pz)), 11.2 (*C*H$_3$(pz)).

Synthesis of the Complexes [$PdCl_2$(L)] [L = L1 (1), L2 (2), L3 (3)]. A CH_3CN solution (20 mL) of [$PdCl_2(CH_3CN)_2$] (70 mg, 0.270 mmol) was added to a CH_3CN solution (5 mL) of the corresponding ligand (103 mg, 0.270 mmol), and the resulting solution was allowed to stir for 12 h at room temperature (**1**), 24 h at 70 °C (**2**), or 168 h at 70 °C (**3**). The solvent was removed in vacuo to yield a yellow solid, which was filtered off, washed with 10 mL of diethyl ether, and dried in vacuum.

1. Yield: 61% (0.092 g). Anal. Calcd for $C_{22}H_{30}Cl_2N_4O_2Pd$: C, 47.20; H, 5.40; N, 10.00. Found: C, 46.99; H, 5.39; N, 9.78. Conductivity (S cm^2 mol^{-1}, 1.15 × 10^{-3} M in CH_3CN): 9.2. MS: *m*/*z* 525.3 (100%) $[M - Cl]^+$. IR (KBr, cm^{-1}): 3131 [ν(C−H)$_{ar}$], 2952, 2868 [ν(C−H)$_{al}$], 1557 [ν(C═C), ν(C═N)$_{ar}$], 1422 [δ(C═C), δ(C═N)$_{ar}$], 1105 [ν(C−O−C)$_{as}$], 793, 757 [δ(C−H)$_{oop}$]. IR (polyethylene, cm^{-1}): 494 [ν(Pd−N)], 335 [ν(Pd−Cl)]. ^{1}H NMR (CD_3CN solution, 250 MHz): δ 7.38 (m, 4H, Ph), 6.03 (s, 2H, C*H*(pz)), 4.95 (t, 4H, ^3J = 7.7 Hz, $N_{pz}CH_2CH_2O$), 4.76 (s, 4H, OCH_2Ph), 4.28 (t, 4H, ^3J = 7.7 Hz, $N_{pz}CH_2CH_2O$), 2.83 (s, 6H, CH_3(pz)), 2.35 (s, 6H, CH_3(pz)). ^{13}C{^{1}H} NMR (CD_3CN solution, 63 MHz): δ 150.9 (pz-*C*), 145.1 (pz-*C*), 138.0−129.4 (Ph), 108.2 (*C*H(pz)), 72.6 (OCH_2Ph), 68.5 ($N_{pz}CH_2CH_2O$), 49.5 ($N_{pz}CH_2CH_2O$), 15.1 (*C*H$_3$(pz)), 11.8 (*C*H$_3$(pz)).

2. Yield: 58% (0.087 g). Anal. Calcd for $C_{22}H_{30}Cl_2N_4O_2Pd$: C, 47.20; H, 5.40; N, 10.00. Found: C, 47.24; H, 5.55; N, 9.79. Conductivity (S cm^2 mol^{-1}, 1.05 × 10^{-3} M in CH_3CN): 8.5. MS: *m*/*z* 525.3 (100%) $[M - Cl]^+$. IR (KBr, cm^{-1}): 3121 [ν(C−H)$_{ar}$], 2919, 2863 [ν(C−H)$_{al}$], 1556 [ν(C═C), ν(C═N)$_{ar}$], 1423 [δ(C═C), δ(C═N)$_{ar}$], 1108 [ν(C−O−C)$_{as}$], 793, 734 [δ(C−H)$_{oop}$]. IR (polyethylene, cm^{-1}): 490 [ν(Pd−N)], 341 [ν(Pd−Cl)]. ^{1}H NMR (CD_3CN solution, 250 MHz): δ 7.25 (m, 4H, Ph), 5.98 (s, 2H, C*H*(pz)), 4.84 (t, 4H, ^3J = 7.3 Hz, $N_{pz}CH_2CH_2O$), 4.62 (s, 4H, OCH_2Ph), 3.93 (t, 4H, ^3J = 7.3 Hz, $N_{pz}CH_2CH_2O$), 2.78 (s, 6H, CH_3(pz)), 2.34 (s, 6H, CH_3(pz)). ^{13}C{^{1}H} NMR (CD_3CN solution, 63 MHz): δ 150.6 (pz-*C*), 144.9 (pz-*C*), 138.4−128.4 (Ph), 108.2 (*C*H(pz)), 72.8 (OCH_2Ph), 67.0 ($N_{pz}CH_2CH_2O$), 49.8 ($N_{pz}CH_2CH_2O$), 15.0 (*C*H$_3$(pz)), 11.6 (*C*H$_3$(pz)).

3. Yield: 49% (0.074 g). Anal. Calcd for $C_{22}H_{30}Cl_2N_4O_2Pd$: C, 47.20; H, 5.40; N, 10.00. Found: C, 47.36; H, 5.19; N, 10.21. Conductivity (S cm^2 mol^{-1}, 1.20 × 10^{-3} M in CH_3CN): 10.6. MS: *m*/*z* 525.3 (100%) $[M - Cl]^+$. IR (KBr, cm^{-1}): 3129 [ν(C−H)$_{ar}$], 2941, 2856 [ν(C−H)$_{al}$], 1556 [ν(C═C), ν(C═N)$_{ar}$], 1423 [δ(C═C), δ(C═N)$_{ar}$], 1103 [ν(C−O−C)$_{as}$], 808 [δ(C−H)$_{oop}$]. IR (polyethylene, cm^{-1}): 486 [ν(Pd−N)], 342 [ν(Pd−Cl)]. ^{1}H NMR (CD_3CN solution, 250 MHz): δ 7.25 (m, 4H, Ph), 6.00 (s, 2H, C*H*(pz)), 4.89 (t, 4H, ^3J = 6.2 Hz, $N_{pz}CH_2CH_2O$), 4.36 (s, 4H, OCH_2Ph), 4.27 (t, 4H, ^3J = 6.2 Hz, $N_{pz}CH_2CH_2O$), 2.81 (s, 6H, CH_3(pz)), 2.33 (s, 6H, CH_3(pz)). ^{13}C{^{1}H} NMR (CD_3CN solution, 63 MHz): δ 151.0 (pz-*C*), 145.6 (pz-*C*), 135.6−129.2 (Ph), 107.8 (*C*H(pz)), 73.2 (OCH_2Ph), 65.0 ($N_{pz}CH_2CH_2O$), 50.0 ($N_{pz}CH_2CH_2O$), 14.8 (*C*H$_3$(pz)), 11.9 (*C*H$_3$(pz)).

Synthesis of the Complexes [$PdCl_2$(L)]$_2$ [L = L1 (4), L2 (5), L3 (6)]. A tetrahydrofuran solution (20 mL) of [$PdCl_2(CH_3CN)_2$] (70 mg, 0.270 mmol) was added to a tetrahydrofuran solution (5 mL) of the corresponding ligand (103 mg, 0.270 mmol), and the resulting solution was allowed to stir for 12 h at room temperature. The solvent was removed in vacuo to yield a yellow solid, which was filtered off, washed with 10 mL of diethyl ether, and dried in vacuum.

4. Yield: 68% (0.103 g). Anal. Calcd for $C_{44}H_{60}Cl_4N_8O_4Pd_2$: C, 47.20; H, 5.40; N, 10.00. Found: C, 47.00; H, 5.58; N, 9.72. Conductivity (S cm^2 mol^{-1}, 1.08 × 10^{-3} M in CH_3CN): 10.1. MS: *m*/*z* 1083.2 (100%) $[M - Cl]^+$. IR (KBr, cm^{-1}): 3130 [ν(C−H)$_{ar}$], 2986, 2865 [ν(C−H)$_{al}$], 1556 [ν(C═C), ν(C═N)$_{ar}$], 1423 [δ(C═C), δ(C═N)$_{ar}$], 1104 [ν(C−O−C)$_{as}$], 791, 755 [δ(C−H)$_{oop}$]. IR (polyethylene, cm^{-1}): 471 [ν(Pd−N)], 352 [ν(Pd−Cl)]. ^{1}H NMR (CD_3CN solution, 250 MHz): δ 7.27 (m, 4H, Ph), 6.01 (m, 2H, C*H*(pz)), 4.91 (m, 4H, $N_{pz}CH_2CH_2O$), 4.47 (m, 8H, OCH_2Ph and $N_{pz}CH_2CH_2O$), 2.76 (m, 6H, CH_3(pz)), 2.29 (m, 6H, CH_3(pz)). ^{13}C{^{1}H} NMR (CD_3CN solution, 63 MHz): δ 150.3 (pz-*C*), 145.0 (pz-*C*), 136.1−128.1 (Ph), 107.8 (*C*H(pz)), 71.2 (OCH_2Ph), 69.3 ($N_{pz}CH_2CH_2O$), 50.0 ($N_{pz}CH_2CH_2O$), 15.1 (*C*H$_3$(pz)), 12.2 (*C*H$_3$(pz)).

5. Yield: 71% (0.108 g). Anal. Calcd for $C_{44}H_{60}Cl_4N_8O_4Pd_2$: C, 47.20; H, 5.40; N, 10.00. Found: C, 47.11; H, 5.23; N, 9.88. Conductivity (S cm^2 mol^{-1}, 1.12 × 10^{-3} M in CH_3CN): 13.2. MS: *m*/*z* 1083.2 (100%) $[M - Cl]^+$. IR (KBr, cm^{-1}): 3129 [ν(C−H)$_{ar}$],

Table 2. Crystallographic Data for Compounds **1** and **4**

	1	**4**
empirical formula	$C_{22}H_{30}Cl_2N_4O_2Pd$	$C_{44}H_{64}Cl_4N_8O_6Pd_2$
fw	559.80	1155.63
temperature (K)	293(2)	293(2)
wavelength (Å)	0.710 73	0.710 73
system, space group	monoclinic, $P2_1/n$	triclinic, $P\bar{1}$
unit cell dimens		
a (Å)	8.173(3)	9.294(11)
b (Å)	22.444(3)	11.198(8)
c (Å)	13.480(4)	13.583(12)
α (deg)	90	90.10(4)
β (deg)	91.89(3)	91.28(4)
γ (deg)	90	104.39(5)
U (Å^3)	2471.4(12)	1369(2)
Z	4	1
D_{calc} (g cm^{-3})	1.505	1.402
μ (mm^{-1})	0.992	0.901
F(000)	1144	592
cryst size (mm^3)	0.2 × 0.1 × 0.1	0.2 × 0.1 × 0.1
hkl ranges	$-11 \le h \le 11$, $0 \le k \le 31$, $0 \le l \le 18$	$-11 \le h \le 11$, $-13 \le k \le 13$, $-17 \le l \le 17$
2θ range (deg)	2.36−29.96	2.56−29.89
reflns collected/unique [R_{int}]	7401/7137 [R_{int} = 0.0528]	10 264/5612 [R_{int} = 0.0434]
completeness to θ (%)	99.3 (θ = 29.96°)	70.9 (θ = 29.89°)
abs corrn	empirical	empirical
data/restrains/param	7137/3/281	5612/22/316
GOF on F^2	1.437	0.711
final R indices [I > 2σ(I)]	R1 = 0.0702, wR2 = 0.1186	R1 = 0.0519, wR2 = 0.1092
R indices (all data)	R1 = 0.1756, wR2 = 0.1775	R1 = 0.1064, wR2 = 0.1184
largest diff peak and hole (e Å^{-3})	0.700 and −0.693	0.918 and −0.413

Table 3. Relative Energies and Selected Dihedral Angles for the Conformers of **4**

	4-I	**4-II**	**4-III**	**4-IV**	**4-V**	**4-VI**	**4-VII**	**4-VIII**
				Relative Energies				
ΔE[a]	0.0	0.6	0.8	2.5	3.4	3.8	3.9	5.8
				Dihedral Angles[b]				
C7−O1	179.4	−169.5	179.2	179.7	−173.9	−179.9	−179.4	78.2
C8−C9	165.8	−177.1	166.2	162.9	177.5	159.7	173.9	−87.3
C14−C15	−170.5	175.7	−78.3	−76.0	−66.5	−75.1	−68.9	−79.9
O2−C16	−161.3	169.5	167.5	111.9	91.7	110.7	88.7	168.5
C16−C17	70.1	−74.4	−80.9	−68.1	70.7	−69.3	74.4	−75.5
C17−N3	75.8	−78.6	−82.1	−77.4	80.1	−76.6	81.5	−81.6
N4−Pd2	69.4	−69.5	−71.5	−69.0	68.5	−66.8	71.9	−69.4
C7′−O1′	−179.4	169.5	−179.3	178.2	−92.9	−83.3	179.1	−78.5
O1′−C8′	−175.6	170.4	−170.1	−174.4	−179.3	−174.6	−176.1	−164.4
C8′−C9′	−165.8	175.9	−165.8	−169.5	67.3	74.1	−173.5	86.6
C14′−C15′	170.5	−177.1	78.3	77.5	163.9	99.1	68.9	80.0
O2′−C16′	161.3	−169.3	−167.1	−121.6	170.6	−162.6	−88.8	−168.4
C16′−C17′	−70.1	74.6	80.8	67.8	−65.7	73.3	−74.1	75.3
C17′−N3′	−75.8	78.9	81.9	77.6	−74.8	80.4	−80.8	81.4
N4′−Pd2	−69.4	70.1	71.2	72.5	−68.6	75.8	−70.0	69.4

[a] Relative to the most stable conformer. In kcal mol^{-1}. [b] Dihedral angles around the specified bonds in degrees. See Figure 8 for atom numbering.

2914, 2863 [ν(C−H)$_{al}$], 1556 [ν(C═C), ν(C═N)$_{ar}$], 1423 [δ(C═C), δ(C═N)$_{ar}$], 1108 [ν(C−O−C)$_{as}$], 791, 729 [δ(C−H)$_{oop}$]. IR (polyethylene, cm^{-1}): 488 [ν(Pd−N)], 355 [ν(Pd−Cl)]. ^{1}H NMR (CD_3CN solution, 250 MHz): δ 7.18 (m, 4H, Ph), 5.98 (m, 2H, C*H*(pz)), 4.87 (m, 4H, $N_{pz}CH_2CH_2O$), 4.45 (m, 4H, OCH_2Ph), 4.36 (m, 4H, $N_{pz}CH_2CH_2O$), 2.75 (m, 6H, CH_3(pz)), 2.28 (m, 6H, CH_3(pz)). ^{13}C{^{1}H} NMR (CD_3CN solution, 63 MHz): δ 150.9 (pz-*C*), 146.3 (pz-*C*), 139.7−127.7 (Ph), 108.2 (*C*H(pz)), 73.2 (OCH_2-Ph), 69.8 ($N_{pz}CH_2CH_2O$), 50.7 ($N_{pz}CH_2CH_2O$), 15.4 (CH_3(pz)), 12.4 (CH_3(pz)).

6. Yield: 75% (0.114 g). Anal. Calcd for $C_{44}H_{60}Cl_4N_8O_4Pd_2$: C, 47.20; H, 5.40; N, 10.00. Found: C, 47.45; H, 5.19; N, 10.22. Conductivity (S cm^2 mol^{-1}, 1.10 × 10^{-3} M in CH_3CN): 12.7. MS: m/z 1083.2 (100%) [M − Cl]$^+$. IR (KBr, cm^{-1}): 3128 [ν(C−H)$_{ar}$], 2919, 2861 [ν(C−H)$_{al}$], 1556 [ν(C═C), ν(C═N)$_{ar}$], 1422 [δ(C═C), δ(C═N)$_{ar}$], 1103 [ν(C−O−C)$_{as}$], 793 [δ(C−H)$_{oop}$]. IR (polyethylene, cm^{-1}): 491 [ν(Pd−N)], 355 [ν(Pd−Cl)]. ^{1}H NMR (CD_3CN solution, 250 MHz): δ 7.26 (m, 4H, Ph), 5.99 (m, 2H, C*H*(pz)), 4.92 (m, 4H, $N_{pz}CH_2CH_2O$), 4.49 (m, 4H, OCH_2Ph), 4.39 (m, 4H, $N_{pz}CH_2CH_2O$), 2.83 (m, 6H, CH_3(pz)), 2.31 (m, 6H, CH_3(pz)) ppm. ^{13}C{^{1}H} NMR (CD_3CN solution, 63 MHz): δ 150.5 (pz-*C*), 145.0 (pz-*C*), 137.8−127.9 (Ph), 107.8 (*C*H(pz)), 73.4 (OCH_2Ph), 69.4 ($N_{pz}CH_2CH_2O$), 50.3 ($N_{pz}CH_2CH_2O$), 15.3 (CH_3(pz)), 12.4 (CH_3(pz)).

X-ray Crystal Structure Analyses of Complexes 1 and 4. Pale-orange single crystals suitable for X-ray analyses were grown by slow diffusion of diethyl ether into a dichloromethane solution of **1** and **4**, respectively. A prismatic crystal was selected and mounted on an Enraf-Nonius CAD4 four-circle diffractometer for **1** and on a MAR345 diffractometer with an image-plate detector for **4**. Unit-cell parameters were determined from automatic centering of 25 reflections (12 < θ < 21°) for **1** and 390 reflections (3 < θ < 31°) for **4** and refined by a least-squares method. Intensities were collected with graphite-monochromatized Mo Kα radiation, using

a $\omega/2\theta$ scan technique. For complex **1**, 7401 reflections were measured in the range $2.36 \leq \theta \leq 29.96$, 7137 of which were nonequivalent by symmetry [R_{int} (on I) = 0.052]. A total of 4292 reflections were assumed, as observed by applying the condition $I \geq 2\sigma(I)$, while for complex **4**, 10 264 reflections were measured in the range $2.56 \leq \theta \leq 29.89$, 5612 of which were nonequivalent by symmetry [R_{int} (on I) = 0.043]. A total of 2472 reflections were assumed, as observed by applying the condition $I \geq 2\sigma(I)$. Lorentz−polarization and absorption corrections were made.

The structure was solved by direct methods, using the *SHELXS* computer program (*SHELXS-97*),[31] and refined by a full-matrix least-squares method with the *SHELXL-97*[32] computer program using 7401 reflections for **1** and 10 264 reflections for **4** (very negative intensities were not assumed). The function minimized was $\sum w||F_o|^2 - |F_c|^2|^2$, where $w = [\sigma^2(I) + 15.2655P]^{-1}$ for **1** and $w = [\sigma^2(I) + (0.0335P)^2]^{-1}$ for **4** and $P = (|F_o|^2 + 2|F_c|^2)/3$. All hydrogen atoms were computed and refined, using a riding model, with an isotropic temperature factor equal to 1.2 times the equivalent temperature factor of the atoms that are linked. The final $R(F)$ factor and $R_w(F^2)$ values as well as the number of parameters refined and other details concerning the refinement of the crystal structure are gathered in Table 2. CCDC 692995 (**1**) and 692996 (**4**) contain the supplementary crystallographic data for this paper. These data can be obtained free of charge from The Cambridge Crystallographic Data Centre via www.ccdc.cam.ac.uk/datarequest/cif.

(31) Sheldrick, G. M. *SHELXS-97, Program for Crystal Structure Determination*; University of Göttingen: Göttingen, Germany, 1997.
(32) Sheldrick, G. M. *SHELXL-97, Program for Crystal Structure Refinement*; University of Göttingen: Göttingen, Germany, 1997.

Acknowledgment. This work has been financially supported by the Spanish Ministerio de Educacion y Cultura (Projects CTQ2007-63913/BQU and CTQ2007-61704/BQU) and by Generalitat de Catalunya (a grant to M.G.). Access to the computational facilities of Centre de Supercomputació de Catalunya (CESCA) is gratefully acknowledged.

Supporting Information Available: Optimized structures of conformers **1-III**, **4-VI**, **4-VII**, and **4-VIII** and Cartesian coordinates of all studied structures. This material is available free of charge via the Internet at http://pubs.acs.org.

IC8013915